

## MACROSCOPIC MODEL ON DRIVER PHYSIOLOGICAL AND PSYCHOLOGICAL BEHAVIOR AT CHANGES IN TRAFFIC

Zawar Hussain Khan<sup>1\*</sup>, T. Aaron Gulliver<sup>2</sup>, Khizar Azam<sup>3</sup>, Khurram Shehzad Khattak<sup>4</sup>

### ABSTRACT

*A model is presented which can accurately characterize macroscopic traffic evolution. This model is based on analogies with the ideal gas law. A traffic constant is proposed which considers both physiological and psychological driver behavior. Physiological behavior is the time taken to observe and process local traffic conditions and then initiate actions while psychological behavior includes the attitude and awareness of a driver. Thus, the traffic constant encompasses the perception, awareness, attitude, and reaction of a driver. The proposed model is evaluated for changes in traffic flow caused by an inactive bottleneck. The results are compared with those for the Payne-Whitham (PW) model. This shows that the temporal and spatial evolution of traffic with the proposed model is more realistic.*

**KEYWORDS:** *Macroscopic traffic, physiological and psychological behavior, Payne-Witham (PW) model, Roe decomposition*

### INTRODUCTION

A new macroscopic model is presented to accurately predict traffic evolution. This model characterizes traffic density and velocity for changes in traffic conditions. Spatial adjustments in traffic are characterized based on driver physiological and psychological behavior. Traffic moves slowly when the density is large as the distances between the vehicles are small. Significant interactions between vehicles occur which cause stop and go traffic. The traffic is more oscillatory over small distances and drivers respond quickly as conditions are more predictable. Faster traffic is observed at low traffic densities as the distances between vehicles are large. In this case, vehicles align to forward conditions independent of nearby vehicles. Due to the presence of large distances between vehicles negligible interactions occur. There are minimal interactions between vehicles in free-flow traffic and driver response is slow. Conversely, during congestion interactions are frequent. In addition, drivers can be sluggish or aggressive based on drug usage, gender, stress, ethnicity, and geographical conditions.

Payne (Payne, 1971) and Witham (Whitham, 1974) (Payne-Witham (PW) model) independently develop macroscopic traffic models based on spatial and temporal traffic evolution. The first equation is a continuity equation which is based on the conservation of vehicles such that no transitions in flow occur and the flow is at equilibrium. The second equation is based on driver

presumption and velocity adjustments (relaxation). The PW model assumes that drivers respond similarly to different conditions and small changes in velocity and density occur (Daganzo, 1995, Khan & Gulliver, 2019). This is an inadequate characterization of driver presumption and as a consequence can result in unrealistic and oscillatory traffic behavior over small distances (Khan et al., 2019).

In this paper, a traffic model is developed using analogies with the ideal gas law which models gas changes due to temperature and pressure. The traffic density changes with velocity, and the velocity is small when the density is high (i.e. during congestion). Conversely, the velocity can be high in free-flow traffic. A traffic constant that characterizes driver physiological and psychological response is proposed which is analogous to the specific gas constant. This response varies based on traffic headway, safe time and velocity. Headway is the distance required for velocity alignment and is related to traffic density. Safe time is the minimum time required for the safe adjustment of velocity and is a function of the velocity. Driver presumption in the anticipation term of the proposed model is based on this traffic constant. Conversely, the anticipation term in the PW model employs a constant velocity to characterize driver response which is unrealistic.

The physiological response is the time required to observe and analyze traffic conditions and then initiate

<sup>1</sup> Department of Electrical Engineering, University of Engineering and Technology, Peshawar

<sup>2</sup> Department of Electrical and Computer Engineering, University of Victoria, Canada

<sup>3</sup> Department of Mechanical Engineering, University of Engineering and Technology, Peshawar

<sup>4</sup> Department of Computer Systems Engineering, University of Engineering and Technology, Peshawar

\*Corresponding author: khanz@uvic.ca

actions. The psychological response considers driver awareness and attitude. The proposed macroscopic traffic model includes both of these responses. Thus, it considers driver perception, awareness, reaction, and attitude. The proposed and PW models are evaluated using a circular (ring) road with an abrupt change in density due to an inactive bottleneck. The results obtained show that traffic behavior with the proposed model is more realistic.

The remainder of this paper is organized as follows. The proposed model is presented in Section II. In Section III, the Roe scheme is employed to implement the PW and proposed models. The traffic behavior with these models is presented in Section IV. Finally, some conclusions are given in Section V.

### PROPOSED TRAFFIC MODEL

The ideal gas law is given by

$$pV=nRT \tag{1}$$

where  $p$  is pressure,  $V$  is volume,  $n$  is the number of moles of gas,  $R$  is the ideal gas constant, and  $T$  is temperature. The number of moles is

$$n = \frac{m}{z}, \tag{2}$$

where  $m$  is the mass and  $z$  is the molar mass. Substituting (2) in (1) gives

$$p = \frac{m}{V} \frac{R}{z} T, \tag{3}$$

The density is  $\rho = \frac{m}{V}$  and the specific gas constant is  $R_s = \frac{R}{z}$ , so that

$$p = \rho R_s T \tag{4}$$

which shows that pressure is proportional to density.

Traffic pressure is analogous to the desire to attain the equilibrium velocity, which is high during congestion and transitions. This effect is similar to the behavior of gas given by (4). Further, the average traffic velocity,  $v$ , is analogous to gas temperature, as an increase in velocity results in greater pressure.

The specific gas constant relates pressure, density, and

temperature. In this paper, a traffic constant  $L_d$  is proposed which relates traffic pressure, density, and velocity. This constant is a function of driver physiological and psychological behavior. Analogous to (4), traffic pressure can be expressed as

$$p = \rho L_d v, \tag{5}$$

The time for a driver to observe traffic conditions and make a decision is known as perception time, where is the density. In congestion, the perception time is large so alignment is slow. Conversely, in free-flow traffic alignment is fast due to the small perception time. Driver attitude can be characterized as the ratio

$$\beta = \frac{\tau_s}{\tau(\rho)}, \tag{6}$$

where  $\tau_s$  is the safe time. Driver behavior is considered normal if the perception time is similar to the safe time. If the perception time is much larger than the safe time, the behavior can be considered sluggish or slow (such as with an intoxicated driver). Conversely, if the perception time is much smaller than the safe time, driver behavior can be considered aggressive. Thus, for a normal driver

$$\beta \approx 1$$

for a slow driver

$$\beta \ll 1$$

and for an aggressive driver

$$\beta \gg 1,$$

The safe time is inversely proportional to the spatial rate of change in velocity  $v_x$  (acceleration), and so can be expressed as

$$\tau_s = \frac{1}{v_x}, \tag{7}$$

where the subscript  $x$  denotes derivative with respect to time. Thus a smaller acceleration or deceleration results in a greater safe time. The perception time  $\tau(\rho)$  is small during free-flow traffic as vehicles align quickly, and is large during congestion. Thus, the perception time due to a change in density can be characterized as

$$\tau(\rho) = \frac{1}{v(\rho)_\rho} \tag{8}$$

where  $v(\rho)$  denotes the equilibrium velocity distribution and the subscript  $\rho$  denotes derivative with respect to density. Substituting (7) and (8) in (6) gives

$$\beta = \frac{v(\rho)_\rho}{v_x} \tag{9}$$

In the literature, driver reaction has been characterized as a constant (Payne, 1971), and also as a linear (Khan et al., 2019) or exponential function of density. While using a constant results in a simple model, it may not provide realistic results. With a linear relationship, the response is too similar in high and low densities. Conversely, with an exponential relationship, significant acceleration and deceleration can occur with high densities, and very low acceleration and deceleration at low densities, which can produce unrealistic behavior. Thus in this paper, the driver reaction is characterized by

$$\rho_x^2 \tag{10}$$

This square law relationship provides a smooth change in traffic flow with variations in density, which is desirable.

Driver awareness increases with greater interaction between vehicles, and so can be characterized by the headway  $S$ . The headway is small during congestion, which increases the acceleration and deceleration, and thus results in more discontinuous traffic flow. Driver awareness increases with density as the surrounding vehicles must be observed more carefully. Conversely, free-flow traffic has a low density, so the headway is large and awareness tends to be low. The traffic headway can then be expressed as

$$S = \frac{1}{\rho} \tag{11}$$

Combining (9), (10), and (11), the traffic constant which characterizes driver response is given by

$$L_d = \frac{v(\rho)_\rho \rho_x^2}{v_x \rho} \tag{12}$$

Several models have been proposed for the equilibrium velocity distribution (Morgan, 2002). The Greenshields model (Greenshields, 1935) is commonly employed

(Muralidharan, 2012) and is given by

$$v(\rho) = v_m \left( 1 - \frac{\rho}{\rho_m} \right), \tag{13}$$

where  $\rho_m$  is the maximum density and  $v_m$  is the maximum velocity. Therefore, (13) is used here to evaluate the traffic models, but other distributions can be employed.

From (5), the rate of change in pressure with respect to density is

$$\frac{dp}{d\rho} = L_d v. \tag{14}$$

The spatial change in pressure is a function of the temporal change in velocity [24], so that

$$\frac{dp}{dx} = -\rho \frac{dv}{dt} \tag{15}$$

Further

$$\frac{dp}{dt} \frac{dt}{dx} = -\rho \frac{dv}{dt}, \tag{16}$$

and substituting  $v = \frac{dx}{dt}$  gives

$$\frac{dp}{dt} = -v\rho \frac{dv}{dt} \tag{17}$$

The temporal change in pressure can also be expressed as

$$\frac{dp}{dt} = \frac{dp}{d\rho} \frac{d\rho}{dt}, \tag{18}$$

and substituting (14) and (17) gives

$$-v\rho \frac{dv}{dt} = L_d v \frac{d\rho}{dt}, \tag{19}$$

The rate of change in  $\rho$  and  $v$  with distance and time is given by

$$\frac{d\rho}{dt} = \frac{\partial \rho}{\partial t} + v \frac{\partial \rho}{\partial x} \text{ and } \frac{dv}{dt} = \frac{\partial v}{\partial t} + v \frac{\partial v}{\partial x} \tag{20}$$

respectively. Then substituting  $\frac{d\rho}{dt}$  and  $\frac{dv}{dt}$  from (20) in (19) gives

$$-\rho(v_t + v v_x) = L_d (\rho_t + v \rho_x), \tag{21}$$

where the subscript  $t$  denotes partial temporal derivative, and  $x$  denotes partial spatial derivative. Adding and

subtracting  $L_d \rho v_x$  to the RHS of (21) gives

$$-\rho(v_t + v v_x) = L_d(\rho_t + (v\rho)_x - \rho v_x), \quad (22)$$

The conservation of vehicles on a road is given by (Lighthill & Whitham, 1955)

$$\rho_t + (\rho v)_x = 0, \quad (23)$$

which models the smooth flow of traffic on a long idealized road. Substituting (23) in the RHS of (22) gives

$$v_t + (v - L_d)v_x = 0, \quad (24)$$

This represents the homogeneous traffic flow as there is no acceleration or deceleration. To include the effect of transitions which result in acceleration or deceleration, a relaxation term is added to the RHS of (24). According to the kinematic equation of motion, acceleration  $a(\rho)$  is given by

$$a(\rho) = \frac{v(\rho) - v}{\tau}, \quad (25)$$

where  $\tau$  is the relaxation time. Considering transitions, (24) can be expressed as

$$v_t + (v - L_d)v_x = \frac{v(\rho) - v}{\tau}, \quad (26)$$

Multiplying by  $\rho$ , the traffic flow is obtained as

$$\rho v_t + \rho(v - L_d)v_x = \rho \frac{v(\rho) - v}{\tau}, \quad (27)$$

The proposed model for traffic flow from (23) and (27) is then

$$\begin{aligned} \rho_t + (\rho v)_x &= 0 \\ \rho v_t + \rho v v_x - \rho L_d v_x &= \rho \frac{v(\rho) - v}{\tau}, \end{aligned} \quad (28)$$

In (28), denotes anticipation. This term includes the traffic constant  $L_d$  which characterizes the driver response.

The PW model (Payne, 1971, Whitham, 1974, Khan, 2016) is

$$\begin{aligned} -\rho L_d v_x \\ \rho v_t + \rho v v_x + \rho C_0^2 \rho_x &= \rho \frac{v(\rho) - v}{\tau}, \end{aligned} \quad (29)$$

where  $C_0$  is the velocity constant which assumes the same driver response for all conditions (Khan et al., 2019, Khan et al., 2019). Thus, driver behavior in the PW model is not dependent on traffic conditions. The relaxation terms in both models are the same as shown in Table I.

**Table 1: Traffic models**

Term	PW model	Proposed model
Anticipation	$\rho C_0^2 \rho_x$	$-\rho L_d v_x$
Relaxation	$\rho \frac{v(\rho) - v}{\tau}$	$\rho \frac{v(\rho) - v}{\tau}$

### ROE TECHNIQUE

In this section, the Roe scheme (Roe, 1981) is applied to evaluate the proposed and PW models. This technique approximates a nonlinear traffic system having flow  $\rho v$  and density  $\rho$  as data variables. This scheme can provide high-resolution results and so can capture abrupt changes in traffic flow. The Roe scheme linearizes the Jacobian matrix of the traffic system by decomposing it into eigenvectors and eigenvalues. This technique can capture large changes in flow and density. The density and flow are obtained as

$$G_i^{n+1} = G_i^n - \frac{\delta t}{\delta x} \left( f_{i+\frac{1}{2}}^n - f_{i-\frac{1}{2}}^n \right) + \delta t S(G_i^n), \quad (30)$$

where  $f_{i+\frac{1}{2}}^n$  denote traffic flow between the boundaries of the  $i$ th and  $(i+1)$ th road segments at the  $n$ th time step,  $\delta t = t_{n+1} - t_n$  is the time step duration,  $G$  is data variables vector and  $S(G_i^n)$  is the source terms vector.

The proposed model (28) in conservation form is

$$\begin{aligned} \rho_t + (\rho v)_x &= 0 \\ (\rho v)_t + \left( \frac{(\rho v)^2}{\rho} - v(\rho)_\rho \rho^2 \right)_x &= \rho \left( \frac{v(\rho) - v}{\tau} \right), \end{aligned} \quad (31)$$

and according to the Roe scheme

$$G = \begin{pmatrix} \rho \\ \rho v \end{pmatrix}, f(G) = \begin{pmatrix} \rho v \\ \frac{(\rho v)^2}{\rho} - v(\rho)_\rho \rho^2 \end{pmatrix}, S = \begin{pmatrix} 0 \\ \rho \frac{v(\rho) - v}{\tau} \end{pmatrix}. \quad (32)$$

From (32), the quasilinear traffic system, i.e.  $\rho \frac{v(\rho) - v}{\tau} = 0$ , is

$$G = \begin{pmatrix} \rho \\ \rho v \end{pmatrix}, f(G) = \begin{pmatrix} \rho v \\ \frac{(\rho v)^2}{\rho} - v(\rho)_\rho \rho^2 \end{pmatrix}, S = \begin{pmatrix} 0 \\ 0 \end{pmatrix}. \quad (33)$$

The Jacobian matrix is then

$$A(G) = \begin{pmatrix} 0 & 1 \\ -v^2 - 2v(\rho)_\rho & \rho 2v \end{pmatrix} \tag{34}$$

The corresponding eigenvalues

$$\lambda_{1,2} = v \pm \sqrt{-(2v(\rho)_\rho \rho)} \tag{35}$$

are used to approximate the traffic flux in (30).

The equilibrium velocity distribution with Greenshields model (13) is a decreasing function of density so

$$v(\rho)_\rho \leq 0, \tag{36}$$

which ensures that the eigenvalues are real and the traffic system is hyperbolic. A hyperbolic system is required such that changes in flow are realistic, unlike the parabolic systems. With

$$v(\rho)_\rho = -\frac{v_m}{\rho_m}, \tag{37}$$

where  $v_m$  is the maximum velocity and  $\rho_m$  is the maximum density, we have

$$\lambda_1 = v + \sqrt{\frac{2v_m \rho}{\rho_m}}, \lambda_2 = v - \sqrt{\frac{2v_m \rho}{\rho_m}}. \tag{38}$$

Thus, the upstream and downstream changes in traffic occur according to the road capacity and maximum velocity at rates  $\lambda_1$  and  $\lambda_2$ , respectively. The corresponding eigenvectors are

$$e_{1,2} = \begin{pmatrix} 1 \\ v \pm \sqrt{\frac{2v_m \rho}{\rho_m}} \end{pmatrix}. \tag{39}$$

The velocity at the boundary of segments  $i$  and  $i+1$  is

$$v_{i+\frac{1}{2}} = \frac{\sqrt{\rho_{i+1}}v_{i+1} + \sqrt{\rho_i}v_i}{\sqrt{\rho_{i+1}} + \sqrt{\rho_i}}, \tag{40}$$

and the corresponding density is

$$\rho_{i+\frac{1}{2}} = \sqrt{\rho_{i+1}\rho_i}, \tag{41}$$

which is the geometric mean at the boundaries. From (40) and (41), the eigenvalues and eigenvectors are

$$\lambda_{1,2} = v_{i+\frac{1}{2}} \pm \sqrt{\frac{2v_m \rho_{i+\frac{1}{2}}}{\rho_m}}, \quad e_{1,2} = \begin{pmatrix} 1 \\ v_{i+\frac{1}{2}} \pm \sqrt{\frac{2v_m \rho_{i+\frac{1}{2}}}{\rho_m}} \end{pmatrix} \tag{42}$$

This indicates that changes in velocity are due to

the average velocity, maximum velocity and maximum density (capacity). A high capacity has smaller changes in velocity compared to with a small capacity. Changes in velocity are larger with a greater  $v_m$ , i.e. faster traffic has greater changes. In congestion, is large and more changes in traffic are observed, resulting in stop and go traffic.

The PW model eigenvalues are

$$\lambda_{1,2} = v_{i+\frac{1}{2}} \pm C_0, \tag{43}$$

so changes in velocity occur at a constant rate regardless of the traffic conditions. The corresponding eigenvectors are

$$e_{1,2} = \begin{pmatrix} 1 \\ v_{i+\frac{1}{2}} \pm C_0 \end{pmatrix} \tag{44}$$

The parameters  $v_{i+\frac{1}{2}}$  and  $\rho_{i+\frac{1}{2}}$  for the PW model are given by (40) and (41), respectively.

Entropy fix is applied to the Jacobian matrix  $A(G_{i+\frac{1}{2}})$  to ensure convergence to a solution at the boundaries (Kermani, & Plett, 2001). The Jacobian matrix is then

$$e|\Lambda|e^{-1}.$$

The diagonal matrix  $|\Lambda| = [\hat{\lambda}_1, \hat{\lambda}_2, \dots, \hat{\lambda}_k, \dots, \hat{\lambda}_n]$  is a function of the eigenvalues  $\lambda_k$ , and  $e$  is the corresponding eigenvector matrix. The Harten and Hayman technique [9] is employed to ensure that is nonnegative.

## PERFORMANCE RESULTS

The performance of the PW and proposed models is evaluated using the parameters shown in Table II. The initial density distribution is

$$\rho_0 = \begin{cases} 0.01, & \text{for } x < 10, \\ 0.3, & \text{for } 10 \leq x \leq 30, \\ 0.1, & \text{for } 30 < x \leq 40, \\ 0.3, & \text{for } 40 < x \leq 50, \\ 0.2, & \text{for } x > 50, \end{cases} \tag{45}$$

which is considered to be worst-case traffic as there are two clusters with significant density variations over a distance of only 100 m. The velocity constant for the PW model varies from 2.4 m/s to 57 m/s depending on the traffic conditions (Morgan, 2002, Jin, 2003, Jin & Zhang, 2001). Thus, the velocity constants considered

here are m/s (Payne, 1971) and m/s. The Greenshields equilibrium velocity distribution is employed with m/s. The relaxation time is s (Imran et al., 2020, Siebel & Mauser, 2006) and the maximum normalized density is . A road step is set to m so there are 100 road steps. The total simulation time is 30 s. The time step for the proposed model is set to s which satisfies the CFL condition (LeVeque, 1992), so the number of time steps is 3000. For the PW model, the time step is set to s with m/s and 0.01 with m/s to satisfy the CFL condition (LeVeque, 1992). The corresponding number of time steps is 30000 for m/s and 3000 for m/s.

Fig. 1 gives the density behavior with the proposed model. This shows that the density changes are greater at 1.5 s than at 15 s and 30 s. At 15 s and 30 s, the traffic is separated into clusters. From 40 to 80 m, the traffic density at s is . The first cluster lies between 8 m and 40 m and has a density which increases from 0.21 at 8 m to 0.28 at 20 m. The density then decreases to 0.18 at 40 m. The second cluster lies between 80 m and 100 m and the density within the cluster changes from 0.17 to 0.21 at 80 m 100 m.

Fig. 2 presents the PW model density behavior with m/s. This shows that there are large changes in density with this model. Further, the traffic divides into 10 closely spaced clusters, each with a span of approximately 9 m. The density within the clusters ranges from 0.08 to 0.3, and the density is very small between clusters. The density behavior of the PW model with m/s is given in Fig. 3. These results show that the abrupt changes in density are smoother at 1.5 s and 15 s. However, at 30 s a density of 2.5 occurs which exceeds the maximum of by a factor of 2.5.

Fig. 4 presents the velocity behavior with the proposed model. This shows that the velocity is more oscillatory at 1.5 s than at 15 and 30 s. At s, the velocity is approximately 28 m/s from 40 m to 80 m The velocity in the first cluster ranges from 25 to 27 m/s, and in the second cluster ranges from 27 to 28 m/s. The velocity evolution is realistic as it stays within the minimum and maximum.

Fig. 5 presents the PW model velocity behavior with 2 m/s. This shows that the velocity oscillates at a lower frequency at 1.5 s than at 15 s and 30 s. At 30 s, the velocity fluctuates from 22.5 to 45.5 m/s even though the

maximum velocity is 34 m. Further, the velocity varies by as much as 20 m/s over a distance of 8 m, which is unrealistic. The PW model velocity behavior with m/s is given in Fig. 6. This shows that at 30 s, velocity goes below zero (-14 m/s) at 68 m, which is not possible.

The proposed model density and velocity behavior over 100 m distance for 30 s is given in Fig. 7 and 8, respectively. These show that the density and velocity with the proposed model evolve realistically. The changes are small and traffic moves faster or slower at locations where the traffic density is low or high, respectively, as expected. The velocity stays within the range of 0 to 34 m/s, and the density between 0 and 1.

The PW model velocity and density behavior with m/s is shown in Fig. 9 and 10 over a distance of 100 m for 30 s, respectively. The velocity varies from 0 m/s to 160 m/s at 0.3 s, which is impossible. Figure 10 shows that the traffic evolves into 10 clusters having a width of approximately 9 m, which is not realistic. The

**Table 2: Simulation parameters**

Parameter	Value
Maximum velocity	$v_m=24$ m/s
Equilibrium velocity distribution	$v(\rho)$
Relaxation time	$\tau=0.5$ s
Anticipation coefficient	$C_0=25$
Road length	$x=100$ m
Time step for the proposed model	$\delta t=0.01$ s
Number of time steps for the proposed model	$N=3000$
Time step for the PW model with $C_0=25$ m/s	$\delta t=0.001$ s
Number of time steps for $C_0=25$ m/s	$N=30000$
Time step for the PW model with $C_0=5.83$ m/s	$\delta t=0.01$ s
Number of time steps for $C_0=5.83$ m/s	$N=3000$
Road step	$\delta x=1$ m
Number of road steps	$M=100$
Simulation time	$t_N=30$ s
Maximum normalized density	$\rho_m=1$

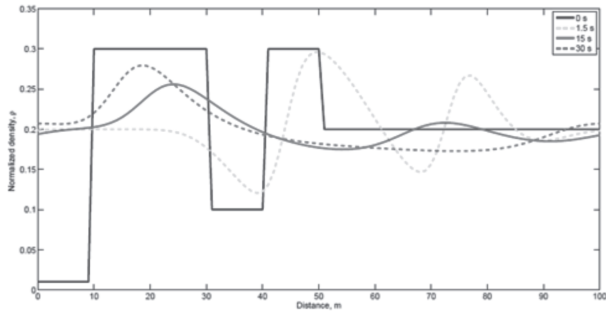


Fig. 1: The density behavior with the proposed model on a 100 m circular at 1.5 s, 15 s, and 30 s.

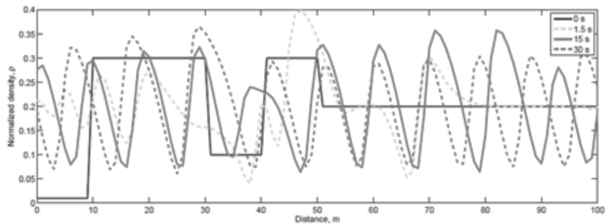


Fig. 2: The density behavior with the PW model for  $C_0=25$  m/s on a 100 m circular road at 1.5 s, 15 s, and 30 s.

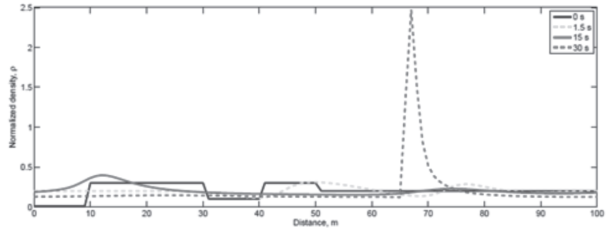


Fig. 3: The density behavior with the PW model for  $C_0=5.83$  m/s on a 100 m circular road at 1.5 s, 15 s, and 30 s

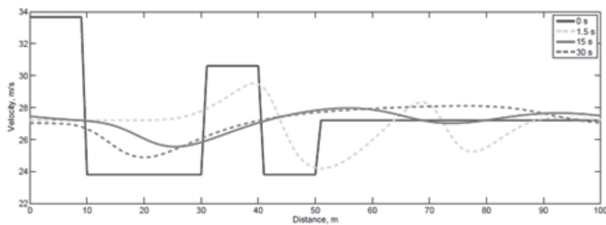


Fig. 4: The velocity behavior with the proposed model on a 100 m circular road at 1.5 s, 15 s, and 30 s.

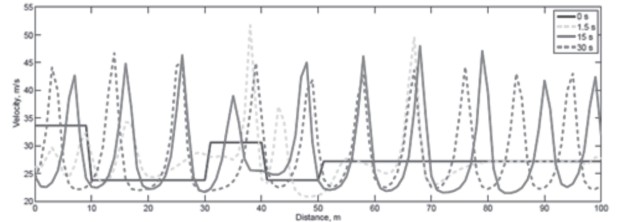


Fig. 5: The velocity behavior with the PW model for  $C_0=25$  m/s on a 100 m circular road at 1.5 s, 15 s, and 30 s.

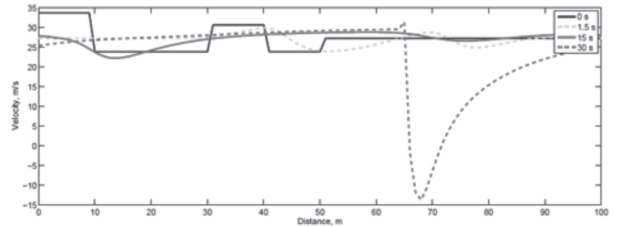


Fig. 6: The velocity behavior with the PW model for  $C_0=5.83$  m/s on a 100 m circular road at 1.5 s, 15 s, and 30 s.

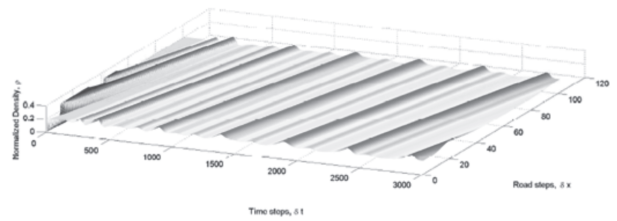


Fig. 7: The density behavior with the proposed model for 30 s on a 100 m circular road.

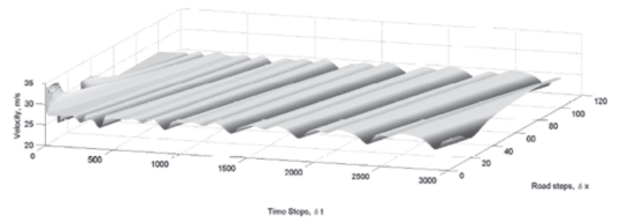


Fig. 8: The velocity behavior with the proposed model for 30 s on a 100 m circular road.

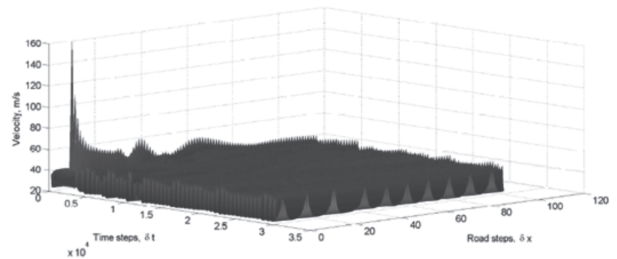
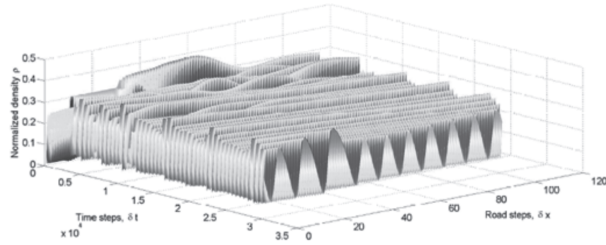
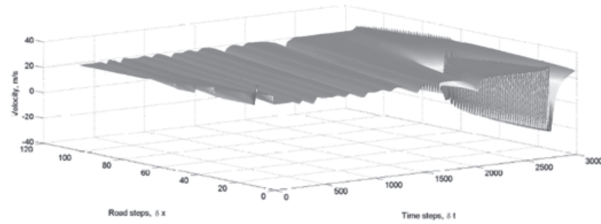


Fig. 9: The velocity behavior with the PW model for  $C_0=25$  m/s and 30 s on a 100 m circular road.



**Fig. 10: The density behavior with the PW model for  $C_0=25$  m/s and 30 s on a 100 m circular road.**



**Fig. 11: The velocity behavior with the PW model for  $C_0=5.83$  m/s and 30 s on a 100 m circular road.**

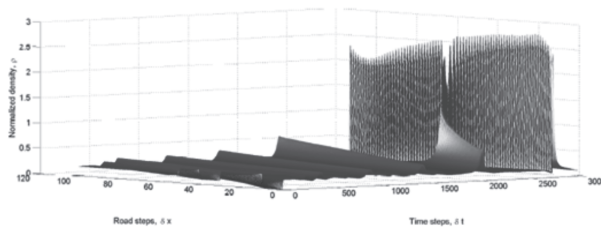


**Fig. 12: The density behavior with the PW model for  $C_0=5.83$  m/s and 30 s on a 100 m circular road.**

corresponding velocity and density behavior with m/s is given in Figures 11 and 12, respectively. These show that the velocity and density oscillations increase with time and distance, so the model is not stable.

The results in this section demonstrate that the proposed model provides realistic traffic behavior which becomes smooth, unlike with the PW model. The PW model produces significant oscillatory behavior with m/s. Further, the oscillations become more pronounced over time whereas they should decrease over time. With m/s, the behavior is also unrealistic. A reason for this is that the PW model does not consider driver response. Conversely, the proposed model produces large initial oscillations due to the large density variations. This oscillatory behavior is due to driver response to the transitions. Over time, these variations decrease as the transitions dissipate. Therefore, the proposed model behavior is more realistic than that of the PW model.

## CONCLUSION

A new traffic model was proposed which is based on the ideal behavior of gas. Analogies with traffic density and velocity were developed. A traffic constant was derived based on driver psychological and physiological behavior. The performance of the proposed model was compared with the well known Payne-Witham (PW) model on a circular road having a traffic bottleneck. Realistic density and velocity behavior were obtained with the proposed model, and it became smooth over time. Further, the density and velocity stayed within the maximum and minimum. These results are due to the use of a proper characterization of the driver response in the model. Conversely, the PW model produced unrealistic behavior for both small and large values of the velocity constant  $C_0$ . The traffic density exceeded the maximum and negative velocities were obtained. Thus, the proposed model is a significant improvement over the PW model.

## FUNDING ACKNOWLEDGEMENT

This project has been supported by the Higher Education Commission, Pakistan, under the establishment of the National Center of Big Data and Cloud Computing.

## REFERENCES

1. Aw A. and Rascle M. (2000), "Resurrection of "second order" models of traffic flow", *SIAM*
2. *Journal Applied Mathematics*, vol. 60, no. 3, pp. 916-938.
3. Bellomo N. and Dogbe C. (2011), "On the Modeling of Traffic and Crowds: A Survey of Models, Speculations, and Perspectives", *SIAM Review*, vol. 53, no. 3, pp. 409-463.
4. Berg P., Mason A. and Woods A. (2000), "Continuum approach to car-following models", *Physics Review E*, vol. 61, no. 2, pp. 1056-1066.
5. Daganzo C. F. (1995), "Requiem for second-order fluid approximations of traffic flow", *Transportation Research B*, vol. 29, no. 4, pp. 277-286.
6. Castillo J. M. D., Pintado P. and Benitez F. G. (1994),

- “The reaction time of drivers and the stability of traffic flow”, *Transportation. Research B*, vol. 28, no. 1, pp. 35-60.
7. Fengchun S., Hui W. and Hong L. (2011), “A mesoscopic model for bicycle flow”, *Proc. Chinese Control Conf.*, pp. 5574-5577, Yantai, China.
  8. Greenshields B. D. (1935), “A study in highway capacity”, *Proceedings of Highway Research Board*, vol. 14, pp. 448-477.
  9. Gupta A. K. and Katiyar V. K. (2006), “A new anisotropic continuum model for traffic flow”, *Physics Review A*, vol. 368, no. 2, pp. 551-559.
  10. Harten A. and Hayman J. M. (1983), “Self adjusting grid methods for one dimensional hyperbolic conservation laws”, *Journal of Computational Physics*, vol. 50, pp. 253-269.
  11. Helbing D. (1995), “Improved fluid dynamic model for vehicular traffic”, *Physics Review E*, vol. 51, no. 4, pp. 3164-3169.
  12. Jin W. (2003), “Traffic flow models and their numerical solutions”, Ph.D. dissertation, Department of Mathematics, University of California, Davis, CA.
  13. Jin W. and Zhang H. M. (2001), “Solving the Payne-Whitham traffic flow model as a hyperbolic system of conservation laws with relaxation”, *Technical Report UCD-ITS-Zhang-2001-1*, University of California, Davis, CA.
  14. Kerner B. S. and Konhuser P. (1993), “Cluster effects in initially homogeneous traffic flow”, *Physics Review E*, vol. 48, no. 4, pp. 2335-2338.
  15. Klar A. and Wegener R. (2000), “Kinetic derivation of macroscopic anticipation models for vehicular traffic”, *SIAM Journal of Applied Mathematics*, vol. 60, no. 5, pp. 1749-1766.
  16. Kachroo P. (2007), “Optimal and feedback control for hyperbolic conservation laws”, Ph.D. dissertation, University of Virginia, Blacksburg, VA.
  17. Khan Z. and Gulliver T. A. (2019), “A macroscopic traffic model based on anticipation”, *Arabian Journal for Science and Engineering*, vol. 44, no. 5, pp. 5151-5163.
  18. Kermani M. J. and Plett E. G. (2001), “Modified entropy correction formula for the Roe scheme”, *American Institute of Aeronautics and Astronautics, Paper 2011-0083*, pp. 1-11.
  19. Lighthill M. J. and Whitham J. B. (1955), “On kinematic waves II: A theory of traffic flow on long crowded roads”, *Proceedings of Royal Society A*, vol. 229, pp. 317-345.
  20. LeVeque R. J. (2nd. Ed.) (1992), “Numerical Methods for Conservation Laws”, *Lectures in Math., ETH Zürich*, Birkhäuser: Basel, Switzerland.
  21. Leer B. V., Thomas J. L., Roe P. L. and Newsome R. W. (1987) “A comparison of numerical flux formulas for the Euler and Navier-Stokes equations”, *American Inst. Aeronautics and Astronautics, Paper 87-1104*, pp. 36-41.
  22. Li T., (2007), “Instability and formation of clustering solutions of traffic flow”, *Bulletin of Institute of Mathematics Academia Sinica (New Series)*, vol. 2, no. 2, pp. 281-295.
  23. Morgan J. V. (2002), “Numerical methods for macroscopic traffic models”, Ph.D. dissertation, Department of Mathematics, University of Reading, Berkshire, UK.
  24. Muralidharan A. (2012), “Tools for modelling and control of freeway network”, Ph.D. dissertation, Department of Mechanical Engineering., University of California, Berkeley, USA.
  25. Nakrachi A., Hayat S. and Popescu D. (2012), “An energy concept for macroscopic traffic flow modeling”, *European Transport. Research. Review.*, vol. 4, no. 2, pp. 57-66.
  26. Payne H. J. (1971), “Models of freeway traffic and control”, *Simulation Council Proceedings*, vol. 1, no. 1, pp. 51-61.

27. Papageorgiou M. (1998), "Some remarks on macroscopic traffic modelling", *Transportation Research A*, vol. 32, no. 5, pp. 323-329.
28. Papageorgiou M., Blosseville J.-M. and Hadj-Salem H. (1990), "Modelling and real-time control of traffic flow on the southern part of Boulevard Peripherique in Paris, Part-1: Modelling", *Transportation Research A*, vol. 24, no. 5, pp. 345-359.
29. Richards P. I. (1956), "Shock waves on the highway", *Operations Research*, vol. 4, no. 1, pp. 42-51.
30. Roe P. L. (1981), "Approximate Riemann solvers, parameter vectors, and difference schemes", *Journal of Computational Physics*, vol. 43, no. 2, pp. 357-372.
31. Strang G. (4th Ed.) (2009), "Introduction to Applied Mathematics", Wellesley: Cambridge Press, MA. 31.  
Tang, T. Q., Huang, H. J., Gao, Z. Y. and Wong, S. C., (2007), "Interaction of waves in the speed-gradient traffic flow model", *Physica A*, vol. 380, no. 1, pp. 481-489.
32. Vorraa T. and Brignone A., (2008), "Modelling traffic in detail with mesoscopic models: Opening powerful new possibilities for traffic analyses", *WIT Trans. The Built Environment*, vol. 101, pp. 659-666.
33. Whitham G. B. (1974), "Linear and Nonlinear Waves", New York: Wiley.
34. Yokoya Y., Asano Y. and Uchida N. (2008), "Qualitative change of traffic flow induced by driver response", *Proceedings of IEEE International Conference on Systems, Man and Cybernetics, Singapore*, pp. 2315-2320.
35. Zhang H. M. (2002), "A non-equilibrium traffic model devoid of gas-like behaviour", *Transportation Research B*, vol. 36, no. 3, pp. 275-290.
36. Zhang H. (1998), "A theory of non-equilibrium traffic flow", *Transportation Research B*, vol. 32, no. 7, pp. 485-498.
37. Khan Z., Gulliver T. A., Khattak K. S. and Qazi, A. (2019), "A macroscopic traffic flow based on reaction velocity", *Iranian Journal of Science and Technology-Transactions of Civil Engineering*, doi:10.1007/s40996-019-00266-y.
38. Khan Z. H., Imran W., Azeem S., Gulliver T. A. and Aslam M. S. (2019), "A macroscopic traffic model based on driver reaction and traffic stimuli", *Applied Sciences*, vol. 9, no. 14, 2848.
39. Khan, Z. Gulliver T.A., Nasir H., Rehman A. and Shahzada K. (2019), "A macroscopic traffic model based on driver physiological response", *Journal of Engineering Mathematics*, vol. 115, no. 1, pp. 21-41.
40. Khan Z., Shah S.A.A. and Gulliver T.A. (2018), "A macroscopic traffic flow model based on weather conditions", *Chinese Journal of Physics B*, vol. 27, no. 7, art. 070202.
41. Khan Z. and Gulliver T.A. (2018), "A macroscopic traffic model for traffic flow harmonization", *European Transport Research Review*, vol. 10, art. 30.
42. Imran W., Khan Z. H., Gulliver T. A., Khattak K. S. and Nasir H., (2020), "A macroscopic traffic model for heterogeneous flow", *Chinese Journal of Physics*, vol. 63, no. 1, pp. 419-435.
43. Siebel F. and Mauser W., (2006), "On the fundamental diagram of traffic flow", *SIAM Journal on Applied Mathematics*, vol. 66, no. 4, pp. 1150-1162.
44. Khan Z. (2016), "Traffic modelling for intelligent transportation systems", Ph.D. dissertation, Department of Electrical and Computer Engineering, University of Victoria, BC, Canada.